AIAA JOURNAL
Vol. 39, No. 3, March 2001

Manufacturability-Based Optimization of Aircraft Structures Using Physical Programming

Michael P. Martinez*
Northeastern University, Boston, Massachusetts 02115
Achille Messac†
Rensselaer Polytechnic Institute, Troy, New York 12180-3590
and
Masoud Rais-Rohani‡
Mississippi State University, Mississippi State, Mississippi 39762

Complex design optimization problems, which involve many nonlinearly coupled design objectives and constraints, pose considerable difficulties in the formulation of the aggregate objective function. A representative example of such a complex optimization problem is the design of aircraft structures based on strength, stiffness, manufacturability, and cost requirements. An effective methodology for such a design has recently been developed. This methodology has been used to develop a computational tool for analysis and optimization of primary structural aircraft components. A wing spar design problem was used to demonstrate the effects of manufacturability and cost requirements on the optimal design configuration. By the use of the computational analysis tool that has been developed, physical programming is applied to the optimization phase of the design. The effectiveness of the physical programming method is demonstrated in the context of such complex problems. In the previous approach, the problem complexity necessitated the minimization of one objective at a time in conjunction with behavioral constraints. The associated Pareto hypersurface is not convex, and the employed approach did not allow the designer to explore the design space efficiently. The use of physical programming is explored for this class of complex problems and it is concluded that physical programming offers the formulation flexibility needed to obtain efficiently the desired points on the Pareto frontier. A comparison with the weighted sum method, as well as the previous results, is made.

I. Introduction

THE design of a complex system usually involves many constraints and objectives (design metrics) and is governed by a number of design parameters that affect these design metrics, typically in a nonlinear fashion. An example of such a multicriteria problem is the design of an aircraft structure that is optimized for performance, as well as manufacturability and cost. This problem could be best defined under the general framework of integrated product and process development and would benefit from more efficient multidisciplinary design optimization solution methods. In this case, manufacturability analysis and cost assessment are integral parts of the design process, which can help to ensure product producibility and affordability at the stage where design choices have the greatest impact on product development.

There are significant challenges associated with design for performance and manufacturability of aircraft structures. A formidable task is the development and implementation of methodologies that can accurately and efficiently address manufacturability and cost requirements (in a quantifiable way) in the design process.[1] In addition, there is a need for efficient optimization techniques that can provide effective design solutions to multicriteria problems with diverse sets of constraints and objectives.

A framework for the design of primary aircraft structures based on strength, stiffness, manufacturability, and cost requirements was developed by Rais-Rohani.[2] In that approach, the manufacturing processes used for each structural part are identified at the beginning of the design process. Cost relationships are established based on the structural definition, material, and process information. The manufacturability factors are used to establish relationships between structural design variables and process parameters in a way that allows for the optimization of the structural system based on performance, as well as manufacturability and cost requirements. This framework was used in the development of a computational tool for preliminary design of aircraft structures based on process information (TASPI). The TASPI framework was subsequently applied to a wing spar design problem[3] to demonstrate the effects of manufacturability and cost requirements in minimizing the weight of the built-up structure.

Multicriteria optimization offers an effective approach for solving such complex engineering problems by providing the designer with the tools to achieve efficient designs while saving time in the decision-making process. The main challenge in multicriteria optimization is the reconciliation of a set of disparate and often conflicting objectives. In such situations, there exists the possibility of attaining numerous Pareto optimal (noninferior, nondominated) solutions. Such solutions arise when there is no other feasible design that will yield an improvement in one objective without causing degradation in another.[4] The collection of these Pareto optimal points forms the Pareto frontier. In practice, the concept of Pareto optimality yields the following question: Once a complex problem is completely defined, how can the desired solutions in the Pareto frontier be obtained? Because of the shortcomings in the formulation of most aggregate objective functions (AOFs), it is very likely that the Pareto solutions cannot all be found.

We briefly comment on the critical common failure to obtain the desired Pareto solution.[4–12] The reasons are twofold. First, formulations of the AOF commonly involve the use of the weighted sum (WS) approach, which uses a linear combination of the design metrics. Unfortunately, this approach only works in the case of convex Pareto frontiers, and structural problems often result in nonconvex Pareto frontiers.[7] Second, even when the Pareto points can be captured in theory, we do not generally know how to set the numerical values of the free parameters, for example, weights in the WS objective function. In addition, as the number of design

Received February 23, 2000; revision received May 30, 2000; accepted for publication July 18, 2000.

*Graduate Student, Multidisciplinary Design Laboratory, Department of Mechanical Engineering.
†Associate Professor, Department of Mechanical Engineering, Aeronautical Engineering and Mechanics; messac@rpi.edu. Associate Fellow AIAA.
‡Associate Professor, Department of Aerospace Engineering.

metrics increases, this task becomes increasingly more difficult, and the proper weights usually cannot be found in reasonable time. The search for the proper weights is often terminated because the designer is sufficiently satisfied with the current solution.

Numerous researchers[4–12] address the related limitations of the WS objective function approach, and physical programming has emerged as an effective alternative to traditional multicriteria design optimization methods. In physical programming (PP), the designer's understanding of the physical problem and desired outcome is exploited in forming the AOF. PP exploits the qualitative perspective of the design optimization process and places this process into a flexible and natural framework that completely eliminates the need for iterative weight settings.

This paper focuses on the application of PP to the multicriteria wing spar design optimization problem, which was investigated previously by Rais-Rohani and Huo[3] using a conventional design optimization scheme. The main objectives are 1) to compare the effectiveness of the PP approach for this class of large structural designs and 2) to examine the Pareto optimal solutions that could not easily (or at all) be obtained using the WS approach. The remainder of this paper is organized as follows. In Sec. II, a wing spar design problem is presented that forms the application basis for this paper. In Sec. III, a synopsis of the PP methodology is provided. In Sec. IV, a PP-based optimization of several wing spar design concepts is presented. These optimization results are compared with those of a previous study of the same concepts. Section IV also includes an instructive comparative study based on the WS optimization approach. Concluding remarks are the subject of Sec. V.

II. Wing Spar Design Problem

This section develops the analytical basis for the wing spar design. In the following, we describe three design concepts that are used for comparative analyses. This description is followed by a brief discussion of the structural and failure analyses, the manufacturability analysis, and the manufacturing cost analysis. The primary objective of our design work is to minimize cost, weight, and tip deflection under prescribed loading. To develop cost relationships, we also address such issues as manufacturability and assembly. We also address strength issues by either imposing constraints or by minimizing appropriate design metrics (on the order of 100 for each concept). In addition, geometrical constraints are imposed on the cap, and appropriate side constraints are enforced.

Description of Three Concepts

The built-up wing spar and loading shown in Fig. 1a forms the basis of our design problem. This structural system consists of a flat web supported by the upper and lower caps, and 21 equally spaced vertical stiffeners. The 20-ft (6.10-m) long spar has a height of 12 in. (30.48 cm) at the root that tapers linearly to 4 in. (10.16 cm) at the tip.

Three different design concepts are considered, as shown in Fig. 1b. In concept 1, each spar cap consists of two identical angle sections with the web sandwiched in between by two rows of fasteners. The flange's length and thickness of each angle section are tapered linearly from root to tip. The web consists of three solid flat sections. Vertical stiffeners are attached on one side of the web at 12-in. (30.48-cm) intervals. These angle stiffeners have joggles at both ends to wrap around the cap flanges. The angle stiffeners are fastened to the web as well as the caps by a single row of rivets.

Concept 2 is similar to concept 1 in terms of web geometry. Each cap consists of a single tee section and is attached to the web with two rows of fasteners. The web stiffeners are attached to the backside of the web and require no joggles. They are attached to the web and caps with a single row of rivets. Concept 3 is identical to concept 2 with one difference. The web in this case consists of three separate pieces spliced together with doubler plates. There is also a circular lightening hole in the web between adjacent web stiffeners for a total of 20 holes. The holes in each of the three web sections are assumed to have the same diameters. The three diameter values are treated as design variables. Each hole also has a 45-deg flange to help stiffen the free edge. The presence of lightening holes makes the web ineffective in bending. Thus, the bending and shear

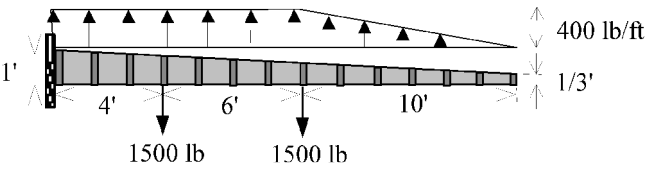

Fig. 1a Spar geometry and loading condition.

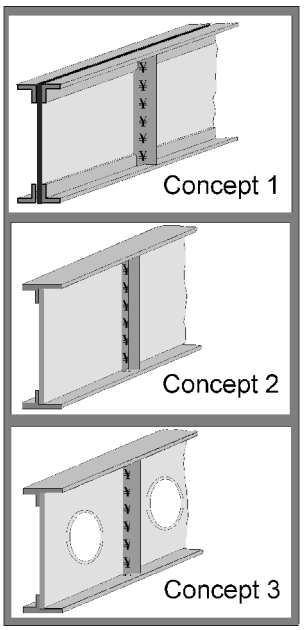

Fig. 1b Detailed views of the three concepts.

loads are assumed to be carried by the caps and the web panels, respectively.

The top caps in all concepts are made of 7075 aluminum extrusion, whereas those at the bottom are made of 2024. The difference in materials accounts for superior fatigue performance of 2024 and high compressive strength of 7075. Because of taper in the caps, machining is used as the primary manufacturing process. The web panels are made of 2024 aluminum sheet. Besides blanking (cutting) the sheet to the correct size (as in concepts 1 and 2), stamping is the primary manufacturing process in concept 3.

All parts are assembled using $\frac{1}{8}$-in.-diam (0.3175-cm) 2017 aluminum fasteners without any sealant. Each concept is produced using a 100% manual bench-top assembly method.

Structural and Failure Analyses

The spar is modeled by a collection of one-dimensional Euler–Bernoulli beam elements with two degrees of freedom per node. Because of taper in the spar, the cross-sectional area and moment of inertia of each element are obtained by averaging the corresponding values at the ends of the element. The tip deflection and the internal load distribution associated with shear and bending loads are based on finite element analysis.

In concepts 1 and 2, the web panels can be loaded up to the buckling state under a combination of shear and bending loads. With the web effective in bending and shear, its failure is based on a bending–shear stress interaction. In concept 3, the web is considered ineffective in bending. Consequently, the caps carry all of the bending loads while the web carries all of the shear loads. In this case, additional requirements are imposed in terms of allowable shear flow in the vicinity of the lightening holes.

The caps are also examined for failure. The compression spar cap is examined for compressive failure in buckling and crippling. The crippling stress can be found by using Gerard's method (see Ref. 2). The Johnson-Euler (see Ref. 2) equation is used to calculate the cap failure stress. The tension spar cap is examined for tensile yielding. The stiffeners are also checked for failure by requiring that the moment of inertia of each stiffener be above the safe minimum.[2] The

Table 1 Manufacturability factors

Compatibility	Complexity	Efficiency
Material–material	Intricacy	Material usage
Material–process	Tolerance and surface finish	Part count
Configuration–process	Nonuniformity	Variety

TASPI analysis software code is used to determine the tip deflection and the margins of safety associated with each failure mode. The details of these analysis capabilities are given in Ref. 2 and are not repeated here.

Manufacturability Analysis

The manufacturability factors considered in this study are listed in Table 1. A complete description of these and other factors can be found in Ref. 2 and are not repeated here. It suffices to point out that simple mathematical relationships are developed by Rais-Rohani[2] to determine the manufacturability index ($\in [0, 1]$) associated with each factor. The total manufacturability index for each concept is a cumulative measure of individual indices, which is used as a key indicator of the manufacturability of each concept. For this calculation, the manufacturability indices for each design concept are combined additively, while treating the factors under compatibility and efficiency as positive and the factors under complexity as negative. For each concept, this scalar sum is divided by the largest possible value for the corresponding concept. The total manufacturability indices for concepts 1, 2, and 3 are found to be 0.6109, 0.6240, and 0.6095, respectively.[2] Therefore, of the three design concepts considered here, concept 2 is deemed the best in terms of manufacturability. For all practical purposes, the total manufacturability index is treated as constant for each concept and not as materially dependent on the design parameters. These indices are primarily useful in comparative studies of the three concepts.

Manufacturing Cost Analysis

Cost estimation models used in this analysis are based on the data provided by the manufacturing cost/design guide (MC/DG).[13] Although these data may not provide highly accurate cost estimates for individual spar designs, they do provide an economic scale by which we can compare different design concepts in terms of relative cost.

Cost estimates consist of both recurring (RC) and nonrecurring (NRC) costs, presented here in terms of labor-hours. The recurring cost usually consists of both labor and raw material costs. The labor costs include those associated with part manufacture and structural assembly, as well as testing, inspection, and evaluation of the assembly and its individual parts. To include the effect of production quantity on recurring manufacturing cost, the labor cost is multiplied by a specific learning curve factor. For sheet metal forming, conventional machining, and bench-top assembly, we use learning curve rates of 90, 90, and 85%, respectively.[14] The learning curve factors to convert unit cost at 200, for instance, to cumulative average cost for 90 and 85% learning curve rates and a quantity of 50 are 1.44 and 1.79, respectively.

Because each spar is a built-up structure with parts mechanically fastened in a 100% manual-assembly process, the effects of the number and type of rivets are considered in the calculation of the assembly cost. If the designed part has features that increase its complexity over the base part, then an additional cost penalty will be included in the recurring cost calculation. Noton[13] defines designer-influenced cost elements (DICE) as joggles, holes, bends, lightening holes, special tolerances, etc., that result in additional cost beyond that for the base part configuration. Because DICE are controlled by the designer, they can be reduced or sometimes eliminated in the design process.

In estimating the recurring cost of each spar design, the cost of raw material was not included. However, the influence of material system on the manufacturing process and associated recurring cost is accounted for through pertinent MC/DG data. The nonrecurring cost consists of two parts. The first is due to tooling and the second to testing, inspection, and evaluation. This cost is separately calculated for the assembly and its individual parts based on MC/DG data. In cases where nonrecurring cost data for a specific manufacturing process were not available, that for comparable processes was used instead.

The equation for manufacturing cost of a discrete part can be expressed in terms of its direct recurring cost (PRC) and nonrecurring cost (PNRC) as[2]

$$\mathrm{DPC} = \mathrm{PRC} + \mathrm{PNRC} \tag{1}$$

where

$$\mathrm{PRC} = (\mathrm{RC}_p + \mathrm{DICE}_p + \mathrm{RC}_{\mathrm{TI\&E}} + \mathrm{DICE}_{\mathrm{TI\&E}})\mathrm{LCF} \tag{2a}$$

$$\mathrm{PNRC} = \mathrm{NRC}_T + \mathrm{NRC}_{\mathrm{TI\&E}} \tag{2b}$$

which includes the recurring labor cost (RC) of manufacturing the base part, RC_p; the additional labor cost of manufacture due to DICE, DICE_p; the RC for testing, inspection, and evaluation (TI&E) of the base part, $\mathrm{RC}_{\mathrm{TI\&E}}$; the additional labor cost of TI&E due to DICE, $\mathrm{DICE}_{\mathrm{TI\&E}}$; the learning curve factor, (LCF), the nonrecurring tooling cost, NRC_T; and the nonrecurring TI&E cost, $\mathrm{NRC}_{\mathrm{TI\&E}}$. All cost terms are presented in units of labor-hours. For a complete manufacturing cost analysis of individual spar parts, see Refs. 2 and 3. The total manufacturing cost (TMC) for a single spar is obtained as[3]

$$\mathrm{TMC} = \sum_i (\mathrm{DPC}_i)(\mathrm{PPS}_i) + \mathrm{TAC} \tag{3}$$

where DPC_i is the manufacturing cost of the ith discrete part, PPS_i is the quantity of ith discrete parts used in the spar assembly, and TAC is the total assembly cost.

This completes the presentation of the analytical model for the wing spar design, which will be optimized using the PP method. A synopsis of this method follows in the next section.

III. Physical Programming Synopsis

Physical programming[15–22] is an optimization method that addresses two critical issues in the case of physical designs that lend themselves to a qualitative and quantitative physical description of the designer's preferences. PP is best discussed in terms of the following steps in the optimization process:

1) Choose design metrics: Based on the current level of knowledge regarding the design artifact, decide which quantities we will care about. We denote the design metrics as $g = \{g_1, g_2, \ldots\}$. (Some may be minimized, whereas others may become behavioral constraints.)

2) Choose design parameters: Again based on the current level of knowledge regarding the desired design, choose the design parameters (the quantities over which the designer has direct control). We denote the design parameters as $x = \{x_1, x_2, \ldots\}$.

3) Develop mapping between design parameters and design metrics: In the process of engineering analysis, the engineer develops a mapping between n design parameters and the m design metrics.

4) Develop AOF: To reflect the design preference with regard to each of the design metrics, the latter are combined to form an AOF.

5) Perform computational optimization: Through the use of any number of possible optimization codes, optimize the AOF formed in step 4, subject to provided constraints.

The important point here is to note that steps 1–3 and 5 involve well-defined tasks for which generally mature procedures exist. This five-step process is only as effective as its weakest link, in this case, step 4. When we have to determine, for example, six weights, and we discover at the conclusion of an unsuccessful optimization run that two of these weights are too small (e.g., 100, 0.01) and one is too large (e.g., 50), we are faced with a truly difficult question. Should we reset these weights at (150, 0.15) and (30) or to some other set of numbers? As we can see, this ad hoc weight-tweaking process can be precarious even for the expert in the field of computational optimization. Bringing efficiency, effectiveness, and user-friendliness to step 4 of the design optimization process is a critical objective of the PP method. For more information concerning the PP method, see Refs. 12, and 15–22. Note that steps 1 and 2 are actually implemented in reverse order at the software level because we need the values of the design parameters to evaluate the design metrics.

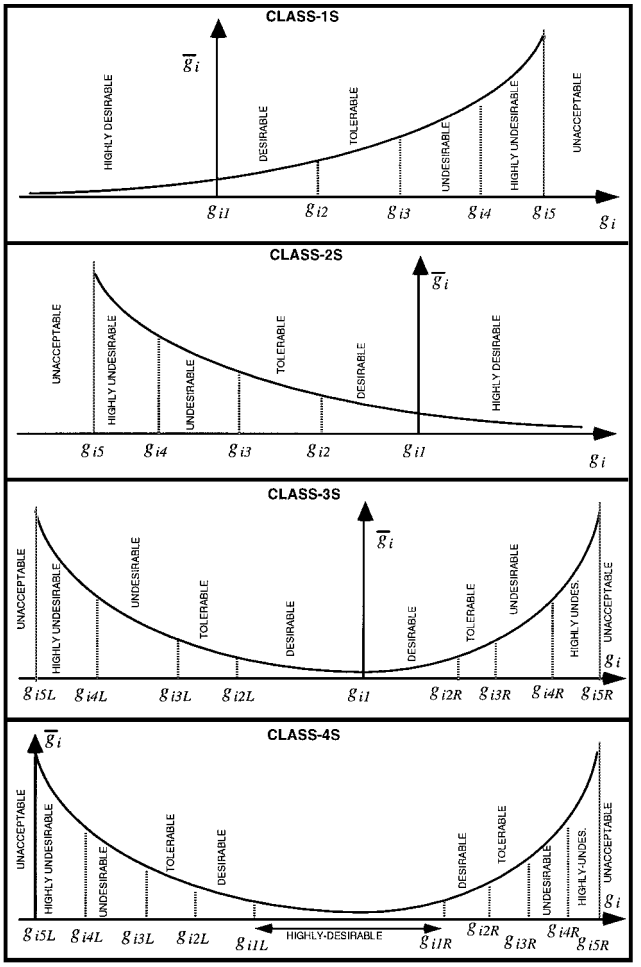

Fig. 2 Class functions for the *i*th generic design metric.

Classification of Design Metrics and Class Functions

Within the PP procedure, the designer expresses preferences with respect to each design metric using four different classes. Each class comprises two cases, hard and soft, referring to the sharpness of the preference. Figure 2 shows the qualitative meaning of each soft class. The value of the design metric under consideration, g_i, is on the horizontal axis, and the function that will be minimized for that metric, $\bar{g}_i$, hereby called the class function, is on the vertical axis. All soft class functions will become constituent components of the AOF. The desired behavior of a generic design metric is, therefore, described by one of eight subclasses, four soft and four hard.

The class functions, shown in Fig. 2, provide the means for a designer to express preferences for each given design metric. Next, we explain how quantitative specifications are associated with each design metric.

PP Lexicon

PP allows the designer to express preferences with regard to each metric with more specificity and flexibility than by simply saying minimize, maximize, greater than, less than, or equal to. The PP lexicon comprises terms that characterize the degrees of desirability: 6 ranges for each generic design metric of classes 1S and 2S, 10 ranges for classes 3S, and 11 ranges for class 4S. Consider, for example, the case of class 1S, shown in Fig. 2. The ranges are defined as follows, in order of decreasing preference: highly desirable range ($g_i \le g_{i1}$), desirable range ($g_{i1} \le g_i \le g_{i2}$), tolerable range ($g_{i2} \le g_i \le g_{i3}$), undesirable range ($g_{i3} \le g_i \le g_{i4}$), highly undesirable range ($g_{i4} \le g_i \le g_{i5}$), and unacceptable range ($g_i \ge g_{i5}$) (this range is treated as infeasible).

The parameters g_{i1}–g_{i5} are physically meaningful constants that are provided by the designer to quantify the preferences associated with the *i*th design metric. These parameters delineate the desirability ranges for each design metric. Further insight into these ranges can be gained by examining the generic shapes of the class functions (Fig. 2). Because the curve in the highly desirable (HD) range is nearly flat, the points in the HD range are of a nearly equivalent desirability level. In other words, in this range, further minimization is not a high priority.

The class functions map design metrics into nondimensional, strictly positive real numbers. This mapping, in effect, transforms design metrics with disparate units and physical meaning onto a dimensionless scale through a unimodal function. Figure 2 shows the mathematical nature of the class functions and shows how they allow a designer to express the preference ranges. Consider the first curve of Fig. 2: the class function for class 1S objectives. Six ranges are defined. The parameters g_{i1}–g_{i5} are specified by the designer. When the value of the design metric g_i is less than g_{i1} (HD range), the value of the class function is small, which requires little further minimization of the class function. When, on the other hand, the value of the metric g_i is between g_{i4} and g_{i5} (highly undesirable range), the value of the class function is large, necessitating significant minimization of the class function. The behavior of the other class functions is indicated in Fig. 2. Stated simply, the value of the class function for each design metric governs the optimization path in objective space for that design metric.

PP Problem Model

With the understanding of the preceding description, the PP problem model takes the following form. For soft classes, perform minimization:

$$\min_x J(x) = \sum_{i=1}^{n_{sc}} \bar{g}_i[g_i(x)] \tag{4}$$

subject to

$$g_i(x) \le g_{i5} \quad \text{(for class 1S objectives)}$$

$$g_i(x) \ge g_{i5} \quad \text{(for class 2S objectives)}$$

$$g_{i5L} \le g_i(x) \le g_{i5R} \quad \text{(for class 3S objectives)}$$

$$g_{i5L} \le g_i(x) \le g_{i5R} \quad \text{(for class 4S objectives)}$$

and, for hard classes invoke constraints,

$$g_i(x) \le g_{iM} \quad \text{(for class 1H objectives)}$$

$$g_i(x) \ge g_{im} \quad \text{(for class 2H objectives)}$$

$$g_i(x) = g_{iv} \quad \text{(for class 3H objectives)}$$

$$g_{im} \le g_i(x) \le g_{iM} \quad \text{(for class 4H objectives)}$$

$$x_{jm} \le x_j \le x_{jM} \quad \text{(for design variation constraints)}$$

where g_{im}, g_{iM}, x_{jm}, and x_{jM} represent minimum and maximum values, the g_{iv} help define the equality constraints, the range limits are provided by the designer (see Fig. 2), and n_{sc} is the number of soft objectives that the problem comprises.

The problem model conforms to the framework of most nonlinear programming codes, with possible minor rearrangements. In this study, we used the software code PhysPro,[21] an advanced implementation of the PP method. Next we turn our attention to the optimization of the design presented in Sec. II.

IV. Design Optimization Problem Definition and Results

This section begins by defining the optimization problem for the design concepts presented in Sec. II. This definition is followed by a presentation and discussion of the PP-based results, which are compared with results from a previous study of the same concepts. The last part of this section discusses the results obtained using the WS approach, and does so within the context of the examination of the Pareto frontier for concept 3.

Optimization Problem Definition for the Three Concepts

The three spar design concepts described earlier (see Fig. 1b) are optimized for minimum weight, manufacturing cost, and tip deflection subject to a set of constraints. In one case, strength constraints are transformed into soft minimized design metrics (class 1S).

Design Variables

In concept 1, the cap is made of two identical angle sections. The vertical and horizontal flange lengths and thicknesses at the root and the tip are used as design variables for a total of eight design variables. The cap dimensions vary linearly from root to tip. The web consists of three sections, each defined by a separate thickness variable (three additional design variables). The web stiffeners are angle sections with two flange length and two thickness design variables (four additional design variables). Thus, concept 1 is governed by a total of 15 design variables.

In concept 2, the cap consists of a single tee section. At the root, the flange comprises a vertical length design variable and two horizontal length design variables (three design variables). To each of these lengths is associated a different thickness design variable (three additional design variables). Linear tapering between root and tip yields an additional 6 design variables at the tip, for a total of 12 design variables. The web and web stiffeners are defined by the same number of design variables as in concept 1. Hence, concept 2 is governed by 19 design variables.

Concept 3 has three additional design variables beyond those in concept 2. These design variables define the size/diameter of lightening holes in each of the three web sections. There are 10 holes in section one (attached to the root), 4 holes in section two, and 6 holes in section three. All holes in a given section have the same diameter. Hence, concept 3 is governed by 22 design variables.

Design Constraints

The strength of various components of the structure is either treated as a design metric to be minimized or as a constraint in nondimensional form expressed as

$$g_s = f_{\text{actual}} / f_{\max} - 1 \tag{5a}$$

for individual structural members. For computational convenience, in the case of minimization, we minimize the worst case:

$$g_{s\max} = \max_i \{g_{s1} \quad g_{s2} \quad \cdots\} \tag{5b}$$

The variable f represents the internal load of interest such as normal stress, shear stress, or shear flow. There are 81 strength design metrics for concept 1, 81 for concept 2, and 101 for concept 3. These strength design metrics address the stress levels in the web, the stiffeners, and the upper and lower caps. As indicated by Eq. (5), the range of g_s is from -1 to 0.

In addition to the strength constraints, we also impose geometrical constraints on the upper and lower caps that generally seek to maintain reasonable aspect ratios and shapes. We have four such constraints for concept 1, and two for concepts 2 and 3. Side constraints are also imposed on the design variables for all three concepts. Geometrical and side constraints are applied in all optimization cases.

Optimization Cases

We describe here the various optimization cases that were considered. Specifically, we describe three cases. Case 1 concerns results from a previous study[3] of the preceding system. Case 2 presents the PP-based results. In case 3, we present a comparative analysis of the results of cases 1 and 2 and of the weighted sum approach.

Case 1 presents results from a previous study.[3] For case 1a, minimize weight, tip deflection $\leq$8 in. (20.32 cm), cost unconstrained, and strength constraints applied. For case 1B, minimize weight, tip deflection $\leq$8 in. (20.32 cm), cost $\leq$95 (labor-hours), and strength constraints applied.

Case 2 presents PP results. For case 2a, minimize weight, cost, and tip deflection, and strength constraints applied: $g_{s\max} \leq -0.001$. For case 2b, minimize weight, cost, and tip deflection; strength design metrics also optimized.

Case 3 involves Pareto frontier generation, weighted sum optimization, PP optimization, comparison of WS and PP results, only concept 3 optimized, and strength constraints applied: $g_{s\max} \leq -0.001$.

Table 2 Optimization results for previous study and PP

Design metrics	Case 1a	Case 1b	Case 2a	Case 2b
		Concept 1		
Weight	47.1	65.2	53.6	54.1
Cost	104.7	95.0	104.6	104.7
Tip deflection	8.0	8.0	7.65	7.60
$g_{s\max}$, see Eq. (5)	−0.00014	−0.0029	−0.0010	−0.0010
		Concept 2		
Weight	45.9	55.1	50.0	50.0
Cost	100.1	95.0	102.0	103.1
Tip deflection	8.0	8.0	7.50	7.50
$g_{s\max}$, see Eq. (5)	0	−0.0037	−0.0010	−0.051
		Concept 3		
Weight	42.3	48.0	49.7	49.7
Cost	101.0	95.0	99.7	99.7
Tip deflection	8.0	8.0	7.34	7.41
$g_{s\max}$, see Eq. (5)	0	−0.00039	−0.0010	−0.0086

Optimization Problem Results for WS and PP

We present the results for all of the optimization cases just defined. We begin with case 1, and follow with cases 2 and 3. The results are summarized in Table 2.

Case 1

The results for case 1 were obtained using the software created in a previous study.[3] The units for weight, cost, and tip deflection are pound, labor-hour, and inch, respectively. The corresponding SI units are shown in parentheses.

Case 1a

In the previous study, the structure's weight was minimized as the sole objective. No attempt was made to seek a tradeoff based on a multiobjective AOF. By examining the nature of the Pareto frontier (Figs. 3 and 4), we will discover why the multiobjective case indeed poses serious difficulties. In this optimization case, the cost is left entirely free. It is not minimized, nor is it constrained. For concept 1 (see Table 2), the minimum possible weight is 47.1 lb (21.36 kg). The tip deflection reaches its upper bound of 8.0 in. (20.32 cm), and the cost reaches a value of 104.7 labor-hour. The maximum value of the strength design metric [Eq. (5)] is -0.00014. The latter was treated, in this case, as an inequality constraint. As we proceed to concepts 2 and 3, the weight decreases to 45.9 and 42.3 lb (20.82 and 19.19 kg), respectively. The cost does not appreciably change from concept 2 to 3.

We note that there is little margin for error/uncertainty because the strength constraint is active. The locations of active strength constraints are 1) the stiffener closest to the root, 2) the upper cap at both locations of the application of the concentrated loads, and 3) the web at the location of the concentrated load farthest away from the root. Therefore, an improved design would allow for these locations to be strengthened. However, the parameterization used in this study does not allow for such a targeted improvement because this is a preliminary study. The strength constraints were active at similar locations in the other cases and concepts. For concept 3, the presence of the lightening holes also resulted in active strength constraints. In conclusion, if the structure's weight is indeed of primordial importance, concept 3 is deemed the best.

Case 1b

In case 1a, the cost was left unconstrained. Case 1b is different in that the cost is constrained to be less than 95 labor-hour. This was done to explore the options available when weight is not the overriding consideration. Table 2 shows the associated results. As expected, for all concepts, cost and tip deflection become active

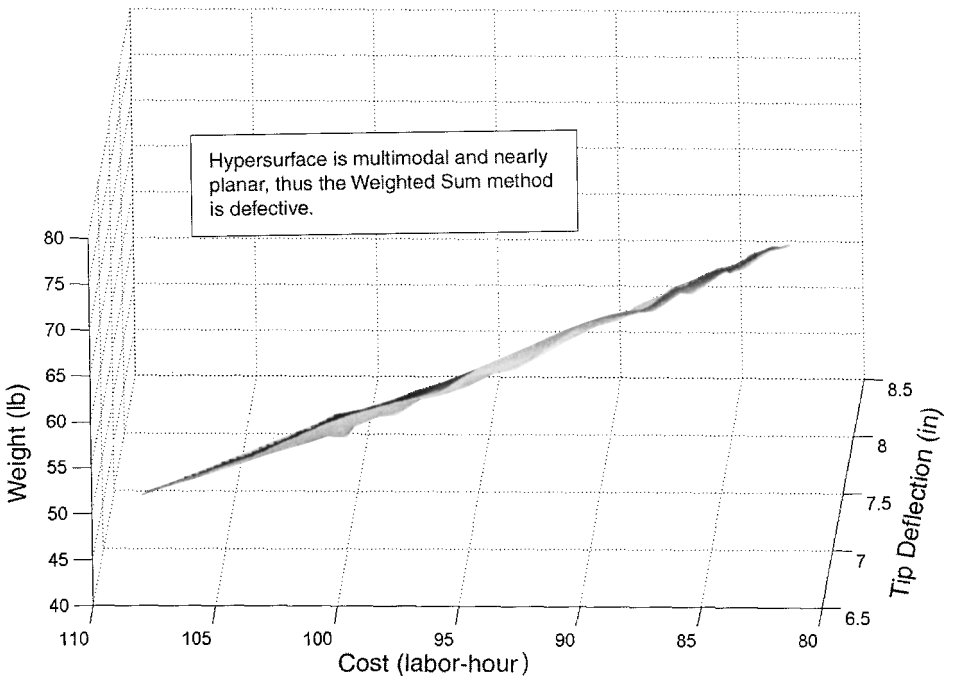

Fig. 3 Design space hypersurface (profile view).

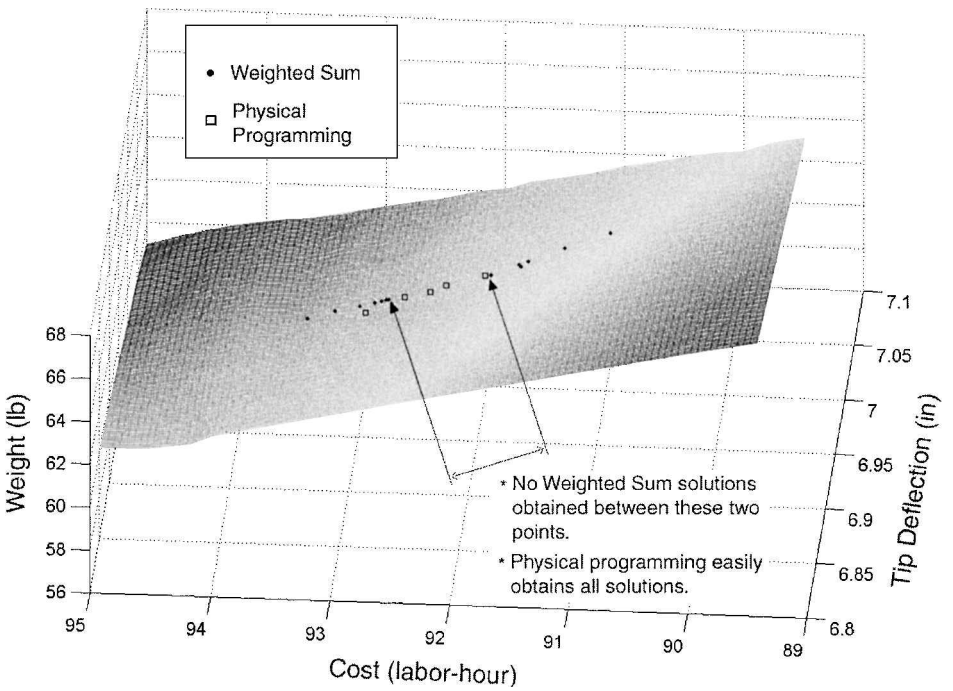

Fig. 4 Design space hypersurface: PP vs WS solutions (perspective view).

constraints. Weight takes on decreasing values of 65.2, 55.1, and 48.0 lb (29.57, 24.99, and 21.77 kg) as we proceed from concept 1 to concept 3. Therefore, if we are only willing to have a cost of 95 labor-hour, then concept 3 is the most appealing. The preceding comments regarding margin for error/uncertainty again apply, if we observe the values of the strength constraints.

From the given results, we observe that this design is truly of a multiobjective nature in that the objectives of interest are strongly in conflict. Therefore, the optimization approach used should adequately model the designer's preferences regarding these objectives (design metrics). It is indeed for these and similar reasons that we have opted to perform this preliminary design optimization using the PP approach, which readily lends itself to identifying the desired tradeoffs among the various design metrics. Case 2 is the subject of this study.

Case 2

The results for case 2 were obtained using PP. We minimized weight, cost, and tip deflection. The preferences used for these design metrics are expressed in the first three rows of numbers in Table 3.

Case 2a

In this case, the strength design metrics are treated as constraints, class 1H. They are not minimized. The results in Table 2 show the tradeoff design that is based on the designer stated preferences in Table 3. The main observation here is that the tradeoff between the tip deflection, the cost, and the weight design metrics is exercised. The tip deflection is now 7.65 in. (19.43 cm) for concept 1, and 7.50 and 7.34 in. (19.05 and 18.64 cm) for concepts 2 and 3, respectively. Both the weight and the cost moderately decrease from concept 1

Table 3 PP designer preferences for each design metric[a]

		HD ⟷	D ⟷	T ⟷	U ⟷	HU ⟷
*i*th Design metric	Class	g_{i1}	g_{i2}	g_{i3}	g_{i4}	g_{i5}
Weight	1S	40	45	50	55	100
Cost	1S	90	95	100	105	120
Tip deflection	1S	7	7.25	7.5	7.75	10
$g_{s\text{-max}}$, see Eq. (5)	1S	−0.1	−0.075	−0.05	−0.025	−0.001

[a]D: desirable, T: tolerable, U: undesirable, and HU: highly undesirable.

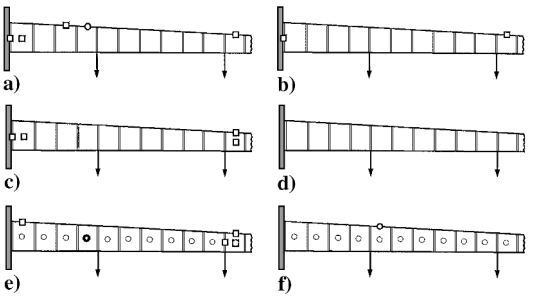

Fig. 5 Strength design metric behavior for PP cases where ○ is moderately stressed ($-0.01 < g_s \leq -0.0025$) and □ is highly stressed ($-0.0025 < g_s \leq -0.001$): a) concept 1, case 2a; b) concept 1, case 2b; c) concept 2, case 2a; d) concept 2, case 2b; e) concept 3, case 2a; and f) concept 3, case 2b.

to 3. Comparing with case 1b, we observe that the decrease in tip deflection is obtained at the expense of increased cost. However, we are not able to predict the trend regarding the weight. The weights of concepts 1 and 2 are lower, whereas that of concept 3 is higher. In conclusion, if we are concerned with the tip deflection level in the manner expressed in the preference table (Table 3), we may conclude that concept 3 is again most desirable. However, in comparison with the results in case 1b, we note that the design of case 2a does not dominate that of case 1b, in the parlance of optimization theory.

This discussion points to the inherent impact of the shape of the Pareto surface and, by implication, of correctly guessing proper scalar weights in forming an AOF. Had we had a well-behaved convex Pareto frontier, our attempt to generate Pareto points by varying weights would have met with more success. Because the Pareto frontier is not of a simplistic nature, the well-known problems with setting weights became particularly glaring. Finally, we note that, here again, there is little margin for error/uncertainty because the strength constraints are active. Figure 5 shows a graphical representation of the strength constraint design metric on the wing spar for case 2a, where we show the highest levels of stress in the structure. In particular, we depict the moderately stressed regions ($-0.01 < g_s < -0.0025$) and the highly stressed regions ($-0.0025 < g_s < -0.001$). This topic will be further discussed after results of case 2b have been presented.

At this point, it is important to realize that the strength constraint might not be entirely appropriate. In fact, the area of robust design[16] explores the consequences of such drastic thinking, as well as the area of reliability analysis (e.g., Ref. 23). Although, in theory, it is best that we design as closely as possible to maximum stress to maximize performance, doing so presents significant pitfalls. First, constraining $g_{s\max}$ [Eq. (5b)] to be simply less than zero leaves no margin for error when there is the slightest uncertainty. As we know, in practice, uncertainties are always present. Second, we do not properly exploit the opportunities that are inherently present in the Pareto surface. For example, we do not know the nature of the tradeoff between the constraint design parameter $g_{s\max}$ and the other design metrics (weight, cost, and tip deflection). Perhaps we are willing to give up some form of performance in exchange for more safety. However, we are reluctant to simply push the safety constraint to some lower number for fear of overdesigning. The direct way to actually express the tradeoff intended in the optimization formulation is to make this constraint design metric $g_{s\max}$ become instead a soft objective (class 1S). The likely alternative would be to make numerous successive optimization runs with different values of each of the constraints (representing diverse constraint combinations). This approach is not practical in most cases. The PP approach offers a direct way of expressing tradeoffs between objectives. In case 2b, we perform exactly this type of optimization. Specifically, we use the preference expressed in the last row of numbers in Table 3 and make $g_{s\max}$ part of the AOF.

We conclude this case by commenting more generally on that we chose to replace the strength constraints by objectives. Simply stated, we wish to recognize that the notion of constraint is more in line with satisfying our need to conform to the necessities of formal mathematical optimization problem formulation than with reality as presented to us. When we prescribe the stress constraint to be <5, we imply that a stress of 4.999 is infinitely good, whereas a stress of 5.0001 is infinitely bad. As we all know, this is not true in practice. In reality, these two values are equally good or bad to us. The major pitfall with using such constraints is that, should the value 5.01 yield a much better overall design, we would have precluded this possibility because it is declared infeasible. Conversely, in the event that we will tolerate the value 4.9, but do not like it very much, the optimization formulation will make no effort to deviate from this not so desirable value. This situation occurs because the inequality constraint is a blunt instrument that entirely fails to reflect the reality of the situation. We use it out of habit and, more important, because it is much easier to handle those objectives (which usually require the setting of weights). Fortunately, PP lends itself to accommodating as many objectives as the designer wishes, so long as there is some idea of what values might be desirable or undesirable.

Case 2b

In this case, the strength design metric $g_{s\max}$ becomes part of the AOF. It is no longer a constraint, as it was in case 2a. Let us compare the results of case 2a with those of the present case 2b. For concept 1, the results have not appreciably changed. This situation results because it is very difficult for the high-stress locations to reduce their stress levels, at least with the design parameter sets used in the optimization. The direct way of alleviating this situation would be to allow for the required mass transfer from one location in the structure to another. With a finer granularity of design parameters in these critical locations, the optimization process would be better equipped to yield appropriate design improvements. As Table 2 shows, the strength constraint is again active.

For concept 2, the situation is more appealing. The strength constraint has significantly improved, and we have paid a relatively minor price. The cost has increased from 102.0 to 103.1 labor-hour. The important point is that the resulting structure is safer, while reflecting the wishes of the designer. Should these results not be to the satisfaction of the designer, it is a simple matter to modify the preferences in Table 3 and do so in a physically meaningful way. We recall that the preference numbers in Table 3 are physically meaningful and that their meanings are clear to the designer. More important, we also note that the results are not unduly sensitive to these input preference numbers. Related issues are addressed by Messac et al.[22]

In the case of concept 3, we merely observe that we have traded the slight worsening of the tip deflection for increased safety of the structure. No other aspect of the structure has appreciably changed. If safety is considered an important factor, in the manner expressed in Table 3, then here again concept 3 is deemed the best. As we see, the strength design metric has improved to -0.009 from -0.001, whereas the tip deflection has increased from 7.34 to 7.41 in. (18.64 to 18.82 cm). In terms of the results of the three concepts for case 2b, we note that the cost for concept 3 is lower because there is a trade that took place between other design metrics. This lower cost was obtained even though concept 3 entails an inherently more expensive manufacturing process, a counterintuitive conclusion. This new finding amplifies the understanding that resulted from the previous study.

Figure 5 shows the status of the strength design metric in various discrete locations of the structure within the context of the moderately stressed and highly stressed definitions. As defined earlier, these locations are as follows. 1) The top line represents the upper cap. 2) The bottom line represents the lower cap. 3) The vertical double lines represent stiffeners. 4) The spaces in between the vertical double lines are the web. Finally, 5) the thinly drawn circular holes in concept 3 represent the lightening holes.

We recall that in case 2a the strength design metric is a constraint (< -0.001, class 1H), whereas in case 2b it is minimized (class 1S). A clear trend can be seen. In case 2b, there are fewer regions where the wing spar is highly stressed. This is true for all three concepts; we will examine concept 3 in particular. In this concept, we observe that from case 2a to case 2b, the structure became at most moderately stressed (see Fig. 5). There is only one moderately stressed region in case 2b, as compared with four highly stressed regions and one moderately stressed region in case 2a. This improvement in the strength constraints, of course, came at some expense to the other design metrics. In particular, there was a degradation of approximately 1% in tip deflection, while weight and cost remained practically unchanged. For concepts 2 and 3, self-explanatory results can also be seen in Fig. 5.

Case 3: Discussion of Pareto Frontier, WS and PP Solutions for Concept 3

We begin with a discussion on the nature of the Pareto frontier associated with this complex nonlinear problem, which will allow us to uncover the associated ramifications. We chose to only perform this analysis for concept 3 because it was the most promising design and, surprisingly, also offered the most complex structure (with lightening holes). Our examining the simplest concept might have led to conclusions of narrower validity. With the aid of the identified section of the Pareto frontier, we perform a comparative analysis of the results obtained using the WS and PP methods. The following results are obtained in conjunction with concept 3.

Pareto frontier examination. The Pareto frontier for concept 3 is generated and shown in Figs. 3 and 4. The surface represents the Pareto frontier pertaining to the three minimizing design metrics (weight, cost, and tip deflection). This frontier was generated to aid in our explanation of the concepts involved. It was generated in the time-consuming fashion of minimizing one objective, while systematically constraining the other two, to generate a fine enough mesh of points to represent the frontier. The strength constraints were set to be less than zero. Figure 3 shows a profile view of the surface, whereas Fig. 4 shows a perspective view. The important associated observations are as follows. 1) Figure 3 shows that the Pareto surface is nearly planar and contains numerous ripples. In particular, the surface is not convex. An immediate consequence of this observation is that if we use the WS approach, we will miss all of the solutions that are in the concave parts of the Pareto frontier. 2) Because the Pareto frontier is nearly planar, a minor change in the numerical weights of the WS formulation will yield a major change in the resulting optimal solution. In other words, this problem/algorithm is numerically ill conditioned, and obtaining the desired design will be difficult. With these observations in mind, we proceed to obtain pertinent numerical results.

Pertinent numerical results on Pareto surface. We begin by examining a restrictive form of the general multiobjective optimization problem, which can be expressed mathematically as

$$\min_{x} g(\boldsymbol{x}) = \begin{bmatrix} g_1(\boldsymbol{x}) \\ g_2(\boldsymbol{x}) \\ \cdot \\ g_N(\boldsymbol{x}) \end{bmatrix} \tag{6}$$

where $\boldsymbol{x}$ is the design parameter vector. The objectives (design metrics) are usually combined to form a single scalar objective function, the AOF, to solve the optimization problem. The AOF is generically written in the form

$$J = \mu[g(\boldsymbol{x})] \tag{7}$$

where μ is a linear or nonlinear function of $g(\boldsymbol{x})$. Examples of the AOF are

$$\mu = \sum_i w_i g_i, \qquad \mu = \sum_i w_i g_i^m$$

in the cases of WS and compromise programming, respectively, where w_i are numerical weights and m is an integer.

In Fig. 4, we show two sets of optimization results, the first using WS and the second using PP. These results are shown on the Pareto surface. The WS results are shown with a circular dot, and the PP results are shown with an empty square. The WS results were obtained by appropriately modifying the associated numerical weights of the AOF. The PP results were obtained using a PP-based method described in Ref. 19.

We make several key observations. First, we note that by varying the weights in the WS approach in an even way, the spread of the solutions is generally quite uneven. This unevenness is in part caused by the surface's multimodality.

Second, the changes in numerical weights of the AOF formulation are extremely small. These numbers are shown subsequently for the leftmost to rightmost points. As we see, these changes occur in the third and fourth significant digits for the second and third numerical weights, respectively, for the first three points. As a result, it is very likely that the designer will obtain solutions at the edge of the Pareto frontier. This is because it is not possible initially to know which sets of weights will yield sensible results. This is because in practice an engineer would not likely vary the weights to this level of precision because of time constraints. The actual weights that had to be used for the weighted sum case are as follows.

Weights for three leftmost point in Fig. 4 (WS):

$$\{w_1, w_2, w_3\} = \{0.0680, 0.0746, 0.8574\}$$

$$\{w_1, w_2, w_3\} = \{0.0680, 0.0747, 0.8573\}$$

$$\{w_1, w_2, w_3\} = \{0.0680, 0.0748, 0.8572\}$$

Weights for rightmost point in Fig. 4 (WS):

$$\{w_1, w_2, w_3\} = \{0.0680, 0.0777, 0.8543\}$$

Third, we see a section of the Pareto surface where no WS solutions could be obtained. Note that nearly exhaustive attempts were made to ensure that such was indeed the case.

Fourth, the PP method has the ability to obtain all Pareto solutions with relative ease.

In comparison with the WS approach, the PP method allows the designer to obtain easily what is desired. This is equivalent to deciding where on the Pareto frontier is most desirable to the decision maker. Finally, theoretical results and applications to date strongly suggest that PP offers the ability of capturing any point on the Pareto frontier. In fact, a formal proof of PP's ability to generate any Pareto point is nearing completion, as of this writing.

V. Conclusions

The PP method was used in the manufacturability-based optimization of an aircraft structure for minimum weight, manufacturing cost, and deflection. By allowing the designer to express preferences regarding each objective in a physically meaningful fashion, PP eliminates the need for tedious and often ineffective weight adjustment process associated with AOF. It was shown that PP is capable of finding optimum solutions that could not be found easily or, in some cases, at all by the WS. This paper showed how the PP method provides a physically meaningful environment to assist designers in their search for the most satisfactory design. These conclusions were reached within the context of the design of three complex wing spar concepts.

Acknowledgment

Support of the National Science Foundation through the CAREER Grant DMI 97-02248 for Achille Messac for part of this work is gratefully acknowledged.

References

[1] Rais-Rohani, M., and Greenwood, A. G., "Product and Process Coupling in Multidisciplinary Design of Flight Vehicle Structures," *Proceedings of the 7th AIAA/USAF/NASA/ISSMO Symposium on Multidisciplinary Analysis and Optimization*, AIAA, Reston, VA, 1998, pp. 897–901.

[2] Rais-Rohani, M., "A Framework for Preliminary Design of Aircraft Structures Based on Process Information," Final Rept., Pts. 1 and 2, NASA Grant NAG-1-1716, Dec. 1998.

[3]Rais-Rohani, M., and Huo, Z., "Analysis and Optimization of Primary Aircraft Structures Based on Strength, Manufacturability, and Cost Requirements," *Proceedings of the 40th AIAA/ASME/ASCE/AHS/ASC Structures, Structural Dynamics, and Materials Conference*, AIAA, Reston, VA, 1999, pp. 1112–1124.

[4]Cohon, J. L., "Multiobjective Programming and Planning," *Mathematics in Science and Engineering*, Vol. 140, Academic Press, San Diego, CA, 1978, p. 168.

[5]Athan, T. W., and Papalambros, P. Y., "A Note on Weighted Criteria Methods for Compromise Solutions on Multi-Objective Optimization," *Engineering Optimization*, Vol. 27, No. 2, 1996, pp. 155–176.

[6]Dennis, J. E., and Das, I., "A Closer Look at Drawbacks of Minimizing Weighted Sums of Objectives for Pareto Set Generation in Multicriteria Optimization Problems," *Structural Optimization*, Vol. 14, No. 1, 1997, pp. 63–69.

[7]Koski, J., "Defectiveness of Weighting Method in Multicriterion Optimization of Structures," *Communications in Applied Numerical Methods*, Vol. 1, 1985, pp. 333–337.

[8]Osyczka, A., *Multicriterion Optimization in Engineering with Fortran Programs*, Series in Engineering, Ellis Horwood, Halsted, NY, 1984, p. 48.

[9]Chen, W., Wiecek, M. M., and Zhang, J., "Quality Utility—A Compromise Programming Approach to Robust Design," *Proceedings of the DETC'98, ASME Design Engineering Technical Conferences*, American Society of Mechanical Engineers, Fairfield, NJ, 1998.

[10]Rakowska, J., Haftka, R. T., and Watson, L. T., "Tracing the Efficient Curve for Multi-Objective Control-Structure Optimization," *Computer Systems Engineering*, Vol. 2, 1991, pp. 461–471.

[11]Das, I., and Dennis, J. E., "Normal-Boundary Intersection: A New Method for Generating the Pareto Surface in Nonlinear Multicriteria Optimization Problems," *SIAM Journal of Optimization*, Vol. 8, No. 3, 1998, pp. 631–657.

[12]Messac, A., Sundararaj, J. G., Tappeta, R. V., and Renaud, J. E., "The Ability of Objective Functions to Generate Points on Non-Convex Pareto Frontiers," *Proceedings of the 40th AIAA/ASME/ASCE/AHS/ASC Structures, Structural Dynamics, and Materials Conference*, AIAA, Reston, VA, 1999, pp. 78–87.

[13]Noton, B. R., "ICAM Manufacturing Cost/Design Guide, Final Technical Report—Airframe User's Manual—Vol. 1 and 3," U.S. Air Force Wright Aeronautical Labs., AFWAL-TR-83-4033, Wright–Patterson AFB, OH, Jan. 1983.

[14]Noton, B. R., "ICAM Manufacturing Cost/Design Guide, Vol. V—Machining," U.S. Air Force Wright Aeronautical Labs., AFWAL-TR-83-4033, Wright–Patterson AFB, OH, March 1985.

[15]Messac, A., "Physical Programming: Effective Optimization for Computational Design," *AIAA Journal*, Vol. 34, No. 1, 1996, pp. 149–158.

[16]Chen, W., Sahai, A., Messac, A., and Sundararaj, G. J., "Exploring the Effectiveness of Physical Programming in Robust Design," *Journal of Mechanical Design*, Vol. 122, June 2000, pp. 155–163.

[17]Messac, A., and Chen, X., "Visualizing the Optimization Process in Real-Time Using Physical Programming," *Engineering Optimization*, Vol. 32, No. 6, 2000, pp. 721–747.

[18]Messac, A., "From Dubious Construction of Objective Functions to the Application of Physical Programming," *AIAA Journal*, Vol. 38, No. 1, 2000, pp. 155–163.

[19]Messac, A., and Sundararaj, G. J., "Physical Programming's Ability to Generate a Well-Distributed Set of Pareto Points," *Proceedings of the 41st AIAA/ASME/ASCE/AHS/ASC Structures, Structural Dynamics, and Materials Conference*, AIAA, Reston, VA, 2000.

[20]Messac, A., "Control-Structure Integrated Design with Closed-Form Design Metrics Using Physical Programming," *AIAA Journal*, Vol. 36, No. 5, 1998, pp. 855–864.

[21]Messac, A., PhysPro Ver. 1.0: Software Package for Optimal Design, Optimal Systems, Latham, NY.

[22]Messac, A., Melachrinoudis, E., and Sukam, C. P., "Mathematical and Pragmatic Perspectives of Physical Programming," *AIAA Journal* (to be published).

[23]Ebeling, C. E., *An Introduction to Reliability and Maintainability Engineering*, McGraw–Hill, New York, 1997, pp. 161–163.

A. Chattopadhyay
Associate Editor